Current-driven threshold switching of a small polaron semiconductor to a metastable conductor

David Emin
Department of Physics and Astronomy, University of New Mexico, Albuquerque, New Mexico 87131, USA
(Received 3 May 2006; published 18 July 2006)

Steady-state current flow through a nonuniform medium generally alters the local carrier density. In particular, driving conventional high-mobility charge carriers through a region in which they collapse into low-mobility small polarons propels the small-polaron density beyond its equilibrium value. There are two contributions to the local augmentation of the small-polaron density. These contributions are proportional to the ratios of the rate governing intersite motion of a conventional high-mobility carrier R_f to (i) the (relatively slow) rate governing intersite hopping of a small polaron R, and to (ii) the (even slower) rate governing conversion of a carrier between being quasifree and being a small polaron, r. As a result of the very large values of these ratios, R_f/R and $R/r \gg 1$, large increases in the small-polaron density can be obtained with accessible electric-field strengths, $<10^6$ V/cm. However, upon being driven to a sufficiently high density, small polarons become unstable with respect to conversion into nonpolaronic carriers. As a result, currents beyond a threshold value can convert a small-polaron semiconductor to a high-mobility semiconductor. Reducing the current permits the material's carriers to relax back to being small polarons. This phenomenon may account for the threshold switching that is observed in materials in which equilibrated carriers appear to form small polarons (e.g., amorphous boron, transition-metal oxide glasses, and chalcogenide glasses).

DOI: 10.1103/PhysRevB.74.035206 PACS number(s): 71.38.Ht, 72.20.Ht, 72.80.Cw, 72.80.Ga

I. INTRODUCTION

Driving a large current through some materials with low electrical conductivity can induce them to switch into a high-conductivity state. The material remains in a high-conductivity state provided current flow is maintained above some minimum value, the *holding* current. If the current drops below the holding value, the material reverts to its low-conductivity electronic transport. This behavior describes the operation of a *threshold* switch.[1–3] Threshold switching is an electronic process. Indeed, switching of small samples is accompanied by very little heating. However, mechanisms for threshold switching are not well established.[1–3]

In some instances, maintaining switched material in its high-conductivity state produces a structural phase transition. After this phase transformation the high-conductivity state persists even in the absence of a holding current. This procedure can result in electronically induced crystallization of an amorphous semiconductor. Then the heating and subsequent rapid cooling that accompanies a suitably engineered current pulse applied to the crystallized material can return a significant portion of it to the amorphous state with its concomitant low conductivity. Such behavior describes the operation of a *memory* switch.[1–3]

Observation of switching behavior began with studies of amorphous boron almost a century ago.[4–7] Switching of transition-metal oxides and organic materials has also been studied.[8] However, most efforts have been directed toward chalcogenide glasses because of their utility in practical devices.[1–3,9]

Studies of steady-state electronic transport of the low-conductivity states of these materials indicate unconventional transport. The predominant charge carriers have been described as small-polarons that move by thermally assisted hopping. In particular, the charge carriers hop between the twelve-atom icosahedral units that comprise amorphous boron,[10] between transition-metal cations in transition-metal oxides,[11] and between lone-pair orbitals on chalcogen atoms (S, Se, and Te) in chalcogenide glasses.[12–16]

Small polarons are distinguished by their hopping transport. As expected for small polarons, Hall mobilities in amorphous As_2Te_3, As_2Se_3, and Sb_2Te_3 are very low, thermally activated, and anomalously signed.[12,13,15–17] Furthermore, the mobility μ that enters into the electrical conductivity is typically considerably smaller than the small-polaron Hall mobility μ_{Hall}: $\mu \approx \mu_{Hall} \exp(-2W_{Hall}/kT)$, where W_{Hall} is the Hall mobility activation energy and kT is the thermal energy.[18,19] Measured values for chalcogenide glasses, including the widely utilized switching material $Ge_2Sb_2Te_5$, $\mu_{Hall} \approx 0.1$ cm^2/Vs and $W_{Hall} \approx 0.05$ eV, yield $\mu \approx 10^{-3}$ cm^2/Vs at 300 K.[13,16,20] Thus, electronic currents in these materials are carried by a high density of low-mobility carriers rather than by a low density of high-mobility carriers.

One may ask: Is threshold switching in these materials associated with their charge carriers being small polarons? Here a mechanism is proposed through which materials with small polarons undergo switching.

The mechanism is based on the small-polaron hopping mobility being orders of magnitude smaller than that of a quasifree carrier of a conventional semiconductor or conductor. Electrical contact to the low-mobility material is made with materials whose carriers have a conventionally high mobility. Steady-state flow then drives an inhomogeneous accumulation of small polarons. The magnitude of this effect increases with the current. With parameters characteristic of threshold switching the small-polaron density of many materials can be pushed high enough to destabilize the small polarons with respect to their conversion into conventional high-mobility carriers. It is this current-driven conversion that is proposed to underlie threshold switching in materials

 ©2006 The American Physical Society

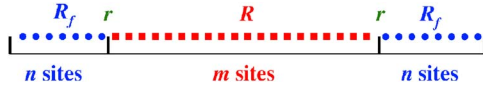

FIG. 1. (Color online) The model envisions a linear chain of m sites upon which carriers self-trap as small polarons. Quasifree carriers enter and exit this chain through two n-member chains. In the absence of a driving electric field, independent small polarons hop between adjacent sites of their chain with the rate R. The field-free rate characterizing quasifree carriers moving between adjacent sites of their n-member chains is denoted by R_f. The rate r characterizes the conversion of a charge carrier between being quasifree and being a small polaron at the boundaries between the two types of chains. The relative magnitudes of these three rates are described by the inequalities: $R_f \gg R \gg r$.

whose equilibrated charge carriers form small polarons.

For clarity a two-state model is used to describe the material that switches. In particular, the material's charge carriers are either quasifree and move with a high-mobility or they form small polarons and execute hopping motion with the concomitant very low mobility. Indeed, charge carriers in covalent systems are understood to manifest such dichotomous behavior.[21–25]

Detailed considerations address a linear chain of m contiguous sites between which carriers move by small-polaron hopping. As illustrated in Fig. 1, quasifree transport occurs in two regions of n sites that bracket the m-member chains: $N=2n+m$.

Three rates enter into this model. Quasifree carriers move between adjacent sites of the n-member chains with the rate R_f. For thermalized free carriers $R_f \sim (WkT)^{1/2}/h$, where W is the carrier's electronic bandwidth and h is Planck's constant. Small polarons hop between adjacent sites of the m-member chain with the rate R. For adiabatic small-polaron hopping $R_f \sim \nu \exp(-W_H/kT)$, where ν is the characteristic atom-vibration frequency and W_H is the hopping activation energy. At the interfaces between regions carriers are slowly converted between being quasifree and being small polarons with the rate r. The maximum value of this rate is $r \sim \nu \exp(-E_b/kT)$, where E_b is the small-polaron binding energy with $E_b > 2W_H$.[26] Near room temperature, where switches typically operate, one generally has $(WkT)^{1/2} > h\nu$ with W being several eV and $h\nu$ being <0.1 eV. As a result, the three pertinent rates customarily satisfy the relationships $R_f \gg R \gg r$.

A steady-state is achieved as an applied electric field drives carriers along the chain. The large disparity in the above-described transition rates ensures that the applied field drives the nonuniform accumulation of small polarons. With a weak field the small-polaron density peaks near where carriers enter the m-member chain. However, with a strong field the peak in the small-polaron density shifts to where small polarons exit the m-member chain. At the electric-field strengths characterizing room-temperature switching ($10^5 - 10^6$ V/cm) the peak fractional enhancement of the small-polaron density is very large, comparable to R_f/r.

Current flow can drive an already high small-polaron density so high that destructive interference between the atomic displacements of different small-polarons can destabilize them with respect to their conversion into quasifree carriers.[23] Above a critical electric field small-polaron-supporting sites along the m-member chain abruptly shrink to a remnant few as chain sites are sequentially destabilized. Thus, a sufficiently strong current can switch a small-polaron semiconductor into a high-conductivity state. The low-conductivity state returns when the current is reduced and carriers relax to form small polarons. These features resemble those of a threshold switch.[1–3]

The bulk of the paper begins in Sec. II with the development of formalism with which to treat non-Ohmic transport and current-driven spatial redistribution of charge carriers along a chain of sites. In Sec. III this formalism is utilized to calculate the electric-field-driven current and spatial redistribution of small polarons along a chain that is connected to two chains whose carriers are quasifree. Numerical estimates of the carrier mobilities and current-driven enhancements of the small-polaron density are given in Sec. IV. In Sec. V the density-driven destabilization of small polarons is explained. Section VI describes how current-driven destabilization of small-polarons produces a threshold switch. Section VII indicates how a structural (e.g., amorphous to crystalline) phase transformation driven by threshold switching results in a memory switch. The paper concludes in Sec. VIII with a summary of the paper's principal arguments and mention of some remaining issues.

II. FORMALISM

Consider charge carriers with charge q moving along a linear chain. The probability of site i being occupied by a carrier is denoted by f_i. Charge transfer occurs between adjacent sites of the chain, where $R_{i,i+1}$ represents the rate with which a carrier can jump from site i to site $i+1$. For simplicity, repulsion between carriers is ignored. Then the current between a pair of sites can be written:

$$\begin{aligned} I_{i,i+1}/q &= f_i R_{i,i+1} - f_{i+1} R_{i+1,i} \\ &= \{\exp[-\beta(\varepsilon_i - \mu_i)]\exp[-\beta(\varepsilon_{i+1} - \varepsilon_i)/2] \\ &\quad - \exp[-\beta(\varepsilon_{i+1} - \mu_{i+1})] \\ &\quad \times \exp[-\beta(\varepsilon_i - \varepsilon_{i+1})/2]\} \times R_0(|\varepsilon_{i+1} - \varepsilon_i|) \\ &= R_0(|\varepsilon_{i+1} - \varepsilon_i|)\exp[-\beta(\varepsilon_i + \varepsilon_{i+1})/2](F_i - F_{i+1}). \end{aligned} \tag{1}$$

In the second line of these equations, the site-occupation factor for site i is expressed

$$f_i = \exp[-\beta(\varepsilon_i - \mu_i)], \tag{2}$$

where β is the reciprocal of the thermal energy $1/kT$. Here k is the Boltzmann constant and T is the absolute temperature. The energy associated with a carrier occupying site i is denoted by ε_i. The site-occupation factor is governed by the quasi-electrochemical potential μ_i, the electrochemical potential in the presence of steady-state current flow. In addition, the rate with which a carrier jumps from site i to site $i+1$ is described with the general expression (Ref. 27):

$$R_{i,i+1} = \exp[-\beta(\varepsilon_{i+1} - \varepsilon_i)/2]R_0(|\varepsilon_{i+1} - \varepsilon_i|). \quad (3)$$

The quasifugacity

$$F_i \equiv \exp(\beta\mu_i) \quad (4)$$

is introduced in the final equality of Eq. (1).

It is now expeditious to exploit the fact that the net difference of the quasifugacity between the ends of the chain can be written as the sum of differences between adjacent pairs of sites. Using this identity along with the above expression for the current between sites i and $i+1$ yields:

$$F_1 - F_N = \sum_{i=1}^{N-1} (F_i - F_{i+1}) = \sum_{i=1}^{N-1} \frac{I_{i,i+1}}{q} \frac{\exp[\beta(\varepsilon_i + \varepsilon_{i+1})/2]}{R_0(|\varepsilon_{i+1} - \varepsilon_i|)} = \frac{I}{q}\sum_{i=1}^{N-1} \frac{\exp[\beta(\varepsilon_i + \varepsilon_{i+1})/2]}{R_0(|\varepsilon_{i+1} - \varepsilon_i|)}. \quad (5)$$

The final expression is obtained upon imposing the steady-state condition that the current be constant, $I_{i,i+1}=I$ for all i.

The generalized impedance for the chain of $N-1$ nearest-neighbor linkages can be defined:

$$Z(m,N) \equiv \frac{1}{\beta q^2}\sum_{i=1}^{N-1} \frac{\exp[\beta(\varepsilon_i + \varepsilon_{i+1})/2]}{R_0(|\varepsilon_{i+1} - \varepsilon_i|)}. \quad (6)$$

In the low-field limit, $F \to 0$, the generalized impedance reduces to just the sum of $N-1$ (electric-field-independent) resistances in series.

The steady-state condition, that there be no net flow of carriers to any site, is now utilized to determine the quasifugacities for sites along the chain. Equating the currents flowing through adjacent pairs of sites yields the relation:

$$\frac{(F_{i-1} - F_i)}{(F_i - F_{i+1})} = \frac{\exp(-\beta\varepsilon_{i+1}/2)R_0(|\varepsilon_{i+1} - \varepsilon_i|)}{\exp(-\beta\varepsilon_{i-1}/2)R_0(|\varepsilon_i - \varepsilon_{i-1}|)} \equiv a_i. \quad (7)$$

The fact that the right-hand side of the equation is positive indicates that the quasifugacity always varies monotonically with position, the site index i. However, the magnitude of the change of quasifugacity with position about site i depends on the magnitude of a_i. For example, $(F_{i-1}-F_i)>(F_i-F_{i+1})$ when $a_i>1$. Furthermore, Eq. (1) indicates that the magnitude of the changes in quasifugacity with position (the site index i) increases with the magnitude of the steady-state current, I.

The quasifugacities along the chain can be computed in a straight-forward manner. In particular, Eq. (7) describes a set of linear relations that link the quasifugacity at a site, F_i, to the quasifugacities at neighboring sites, F_{i-1} and F_{i+1}. There are $N-2$ such equations for a chain of N sites. In addition, boundary conditions establish the quasifugacities at the sites at the two ends of the chain, F_1 and F_N.

Here an algebraic identity is exploited to obtain an expression for the quasifugacity at site s, F_s:

$$F_s - F_N = \sum_{i=s}^{N-1} (F_i - F_{i+1}) = \left(1 + \sum_{i=s}^{N-2}\prod_{j=i}^{N-2} a_{j+1}\right)(F_{N-1} - F_N) = \frac{\left(1 + \sum_{i=s}^{N-2}\prod_{j=i}^{N-2} a_{j+1}\right)}{\left(1 + \sum_{i=1}^{N-2}\prod_{j=i}^{N-2} a_{j+1}\right)}(F_1 - F_N). \quad (8)$$

The quasifugacity at site s is then written as follows:

$$F_s = \frac{F_1 G(s) + F_N[G(1) - G(s)]}{G(1)}, \quad (9)$$

where

$$G_s \equiv 1 + \sum_{i=s}^{N-2}\prod_{j=i}^{N-2} a_{j+1}, \quad (10)$$

and boundary conditions set the values of F_1 and F_N.

The density of carriers at site s is then given by

$$n_s = \exp(-\beta\varepsilon_s)F_s. \quad (11)$$

Application of an electric field alters ε_s while the attendant current flow alters F_s. Electric-field-induced charge accretion and depletion occurs when these two effects fail to cancel one another. In particular, charge accretion and depletion generally occurs near the boundaries between regions with disparate charge transport. The electric-field-induced carrier redistribution associated with a steady-state electric current passing between regions with quasifree carriers and self-trapped carriers is addressed below.

III. TWO-STATE MODEL

Charge transport along the linear chain described by Fig. 1 is now addressed. The chain of Fig. 1 comprises three components. Charge carriers self-trap to form small polarons on the m-member central portion of the chain. Quasifree charge carriers enter and exit the m-member chain from the two n-member chains that adjoin it. Thus the total linear chain comprises $N \equiv m+2n$ sites.

To focus on the essentials of the switching process, nonessential energetic variations are ignored. In particular, energetic disorder among each of the two classes of site is disregarded. Thus, the energy associated with each site at which self-trapping occurs is $-E_b - qFa(i-1)$, where E_b is the small-polaron binding energy and q denotes a carrier's charge while F and a denote the strength of the applied electric field and the intersite separation, respectively. Analogously, the energy associated with each site at which self-trapping does not occur is $-E_f - qFa(i-1)$, when E_f is the lowering of an untrapped carrier's energy associated with its transfer to adjacent sites. It is convenient to define $\Delta \equiv E_f - E_b$.

There are three different charge transfer processes. These processes are each characterized by a different rate function R_0 as introduced in Eq. (3). For intersite transfer among sites with self-trapping this rate function is defined by $R_0 \equiv R$. For

quasifree motion between sites the rate function is defined by $R_0 \equiv R_f$. The rate function for transitions between the self-trapped and quasifree states is described by $R_0 \equiv r$.

The coefficients defined by the condition of steady-state flow in Eq. (7) can now be expressed in terms of the parameters of the two-state model. Within this model the value of a_s at a site bounded by sites with identical charge transport is $A \equiv \exp(\beta qFa)$. For a site supporting quasifree transport that borders a site supporting self-trapping for $i > s$, $a_s = AB$, where $B \equiv \exp(-\beta\Delta/2)(r/R_f)$. At the adjacent site which supports self-trapping, $a_s = AC$, where $C \equiv \exp(-\beta\Delta/2)\ (R/r)$. For a self-trapping site s that borders a region which supports free-carrier transport for $i > s$, $a_s = A/C$. At the adjacent site, the quasifree site along the border $a_s = A/B$. Thus, a bilayer characterizes each interface between the region of self-trapped transport and each of the two regions of quasifree transport that surround it.

A. The generalized impedance

The electric-field dependence of the steady-state current can be obtained by evaluating the generalized impedance. The summation in the expression for the generalized impedance can be evaluated for this model with the aid of the algebraic formula

$$\sum_{j=0}^{M-1} b^j = \frac{1 - b^M}{1 - b}. \tag{12}$$

After straightforward but lengthy manipulations, the generalized impedance can be written as the sum of five contributions that are each associated with successive regions along the chain. Region 1 supports quasifree transport. Region 2 comprises the passage from a site identified with quasifree transport to one identified with small-polaron hopping. Transport in region 3 is by small-polaron hopping. Region 4 denotes the transition from a site that supports small-polaron formation to the adjacent site that is associated with quasifree motion. Region 5 is a region with quasifree transport. The generalized impedance is:

$$Z(m,N) = \frac{1}{2\beta q^2 \sinh(\beta qFa/2)}(L_1 + L_2 + L_3 + L_4 + L_5), \tag{13}$$

where

$$L_1 \equiv \frac{\exp(-\beta E_f)}{R_f}\{1 - \exp[-\beta qFa(n-1)]\}, \tag{14}$$

$$L_2 \equiv \frac{\lfloor -\beta(E_b + E_f)/2 \rfloor}{r}[1 - \exp(-\beta qFa)]\exp[-\beta qFa(n-1)], \tag{15}$$

$$L_3 \equiv \frac{\exp(-\beta E_b)}{R}\{\exp(-\beta qFan) - \exp[-\beta qFa(n+m-1)]\}, \tag{16}$$

$$L_4 \equiv \frac{\lfloor -\beta(E_b + E_f)/2 \rfloor}{r}[1 - \exp(-\beta qFa)] \times \exp[-\beta qFa(n+m-1)], \tag{17}$$

and

$$L_5 \equiv \frac{\exp(-\beta E_f)}{R_f}\{\exp[-\beta qFa(n+m)] - \exp[-\beta qFa(N-1)]\}. \tag{18}$$

When small polarons' slow motion provides the limiting contribution to the generalized impedance the predominant contribution comes from L_3. Then, the generalized impedance of the chain becomes

$$Z(m,N) = \exp(-\beta qFan)\frac{\exp(-\beta E_b)}{2\beta q^2 R \sinh(\beta qFa/2)} \times \{1 - \exp[-\beta qFa(m-1)]\}. \tag{19}$$

The generalized impedance (i) falls with increasing electric-field strength, (ii) rises non-linearly with m, and (iii) depends on the position of the m-site small-polaron subchain (labeled by n) within the N-site chain. The factor $\exp(-\beta qFan)$ is associated with accumulation of carriers about the interface at which carriers enter the region with small-polaron transport. In the customary situation $n \to 0$ as the applied electric field is taken to be applied only over the sites of the m-site chain.

In the limit of small electric field, the generalized impedance reduces to the impedance associated with ohmic conduction. In particular, the impedance then becomes (1) independent of the electric-field strength, (2) simply proportional to the number of equivalent links of the small-polaron portion of the chain, $m-1$, and (3) independent of the position of the m-site small-polaron subchain within the N-site chain:

$$Z(m,N) \to \frac{\exp(-\beta E_b)}{\beta q^2 R}(m-1). \tag{20}$$

Equation (20) gives the established result for ohmic small-polaron hopping on a chain of $m-1$ equivalent links.[26] In the nonohmic high-field regime the electric field dependence of the current is proportional to that of the inverse generalized impedance: $I \propto 1/Z(m,N) \propto \sinh(\beta qFa/2)$. For simplicity, the dependence of R on the electric-field strength has been ignored since it is relatively weak. For example, since $R \propto \exp[-\beta(qFa)^2/8E_b]$ for high-temperature small-polaron hopping, the electric-field dependence of R is much weaker than that of $\exp(-\beta qFa)$ when $qFa < E_b$, as assumed herein.[26]

The contributions to the generalized impedance from the interfaces between regions with quasifree transport and small-polaron transport are associated with L_2 and L_4:

$$Z_{interfacial}(m,N) = \frac{\lfloor -\beta(E_b + E_f)/2 \rfloor}{\beta q^2 r}[1 + \exp(-\beta qFam)] \times \exp[-\beta qFa(n - 1/2)]. \tag{21}$$

The generalized impedance from the two interfaces depends

upon their locations along the N-member chain and upon the electric-field strength, F. However, in the low-field limit, $F \to 0$, where conduction becomes ohmic, the net interfacial impedance reduces to just the sum of that from two equivalent interfaces:

$$Z_{interfacial}(m,N) = 2\frac{\lfloor -\beta(E_b+E_f)/2 \rfloor}{\beta q^2 r}. \tag{22}$$

B. Quasifugacity

The quasifugacity at a site along the chain can be obtained for the two-state model. To begin, the function $G(s)$ of Eq. (10) is evaluated. Considerable straightforward algebraic manipulation yields the following results. In the region with quasifree carriers, $N \geqslant s \geqslant n+m+2$:

$$G(s) = \frac{1-A^{N-s}}{1-A}. \tag{23}$$

At site $n+m+1$, the interface between the region with quasifree carriers and self-trapped carriers:

$$G(n+m+1) = \frac{1-A^{N-n-m-2}}{1-A} + \frac{A^{N-n-m-2}}{B}. \tag{24}$$

In the region with self-trapped carriers, $n+m \geqslant s \geqslant n+2$ with $m \geqslant 2$:

$$G(s) = \frac{1-A^{N-n-m-2}}{1-A} + \frac{A^{N-n-m-2}}{B} + \frac{A^{N-n-m-1}}{BC}\frac{1-A^{n+m+1-s}}{1-A}. \tag{25}$$

At site $n+1$, the interface between regions with self-trapped carriers and quasifree carriers:

$$G(n+1) = \frac{1-A^{N-n-m-2}}{1-A} + \frac{A^{N-n-m-2}}{B} + \frac{A^{N-n-m-1}}{BC}\frac{1-A^{m-1}}{1-A} + \frac{A^{N-n-2}}{B}. \tag{26}$$

Finally, in the region with quasifree carriers, $n \geqslant s \geqslant 1$:

$$G(s) = \frac{1-A^{N-n-m-2}}{1-A} + \frac{A^{N-n-m-2}}{B} + \frac{A^{N-n-m-1}}{BC}\frac{1-A^{m-1}}{1-A} + \frac{A^{N-n-2}}{B} + A^{N-n-1}\frac{1-A^{n-s+1}}{1-A}. \tag{27}$$

In the limit of a uniform chain, $B=C=1$, $G(s)$ reduces to a simple form:

$$G(s) = \frac{1-A^{N-s}}{1-A} \tag{28}$$

for $N \geqslant s \geqslant 1$. Inserting this expression into that for the quasifugacity, Eq. (9), with imposition of the boundary conditions,$F_1=1$ and $F_N=A^{1-N}$, yields

$$F_s = A^{1-N}\left[1 + \frac{A^{N-s}-1}{A^{N-1}-1}(A^{N-1}-1)\right] = A^{1-s}. \tag{29}$$

As described by Eq. (11), the electric-field dependence of the carrier density is the product of that of the quasifugacity, A^{1-s} and that of $\exp(-\beta\varepsilon_s)$, proportional to $\exp[\beta qFa(s-1)] = A^{s-1}$. Thus, these formulae confirm that the local carrier density is independent of the electric-field strength for steady-state flow along a uniform chain.

C. Flow induced carrier redistribution

Current flow induces a redistribution of charge carriers along a nonuniform chain. In particular, the occupation probability for small-polarons at site s relative to its electric-field-free $(A=1)$ value is given by

$$g_s = A^{s-1}F_s = A^{s-1}\frac{F_1 G(s) + F_N[G(1)-G(s)]}{G(1)} = A^{s-1}\frac{G(s) + A^{1-N}[G(1)-G(s)]}{G(1)}, \tag{30}$$

upon imposition of the boundary conditions, $F_1=1$ and $F_N = A^{1-N}$. As above, the electric-field dependent contribution to the energy of a small-polaron at site s is given by A^{1-s}. It is easily verified that the charge redistribution induced by steady-state current flow vanishes ($g_s=1$ for all s) in the absence of an applied electric field $(A=1)$.

The relative occupation probabilities in the region in which carriers self-trap, between site $n+1$ and site $n+m$, for the two-state model are obtained by combining Eqs.(25)–(27) and (30):

$$g_{n+1} = \frac{1-A^{2n-2} + \frac{A^{2n-2}}{B}(1+A^m)(1-A) + \frac{A^{2n-1}}{BC}(1-A^{m-1})}{1-A^{n-2} + \frac{A^{n-2}}{B}(1+A^m)(1-A) + \frac{A^{n-1}}{BC}(1-A^{m-1}) + A^{n+m-1}(1-A^n)}, \tag{31}$$

and

$$g_s = \frac{A^{s-n-1} - A^{s+n-3} + \frac{A^{s+n-3}}{B}(1-A)(1+A^{1-2n}) + \frac{1}{BC}(1 - A^{s-n-2} + A^{s+n-2} - A^{2n+m-1})}{1 - A^{n-2} + \frac{A^{n-2}}{B}(1+A^m)(1-A) + \frac{A^{n-1}}{BC}(1-A^{m-1}) + A^{n+m-1}(1-A^n)} \quad (32)$$

for $n+m \geqslant s > n+1$. Straightforward algebraic evaluation confirms that $g_{n+1}=1$ and $g_s=1$ when $B=C=1$ and that $g_{n+1} \rightarrow 1$ and $g_s \rightarrow 1$ as $A \rightarrow 1$.

To eliminate effects arising from proximity of the m-member chain to the most-distant edges of the n-member chains, proceed to the limit of a finite-size chain of m sites symmetrically embedded within an arbitrarily long chain of $2n+m$ sites ($n \rightarrow \infty$). The relative occupation probability for site u along the m-member chain then becomes:

$$f_u = \left(\frac{1}{B} - \frac{1}{BC}\right)(1 - A^{-1})\delta_{u,1} + \left(\frac{1}{B} - 1\right)(1 - A^{-1})A^{u-m-1} + \left(\frac{1}{BC} - 1\right)(1 - A^{u-m-1}), \quad (33)$$

where $u \equiv s-n$ with $m \geqslant u \geqslant 1$, $f_u \equiv g_{n+u}-1$ in the limit that $n \rightarrow \infty$, and $\delta_{u,1}$ is the Kronecker delta, unity for $u=1$ and zero otherwise. The flow-induced enhancement of the small-polaron density given by Eq. (33) vanishes as the driving field vanishes ($f_u \rightarrow 0$ as $A \rightarrow 1$) and saturates as the driving field becomes arbitrarily large ($f_u \rightarrow 1/BC-1$ as $A \rightarrow \infty$). In addition, the second contribution to the r.h.s. of Eq. (33) peaks at $(1/B-1)/4$ when $u=m$ and $A=2$. This contribution will be seen to be of paramount importance for switching.

In the presence of a driving field, $A > 1$, carriers accumulate, $f_1 > 1$, as they enter the chain at $u=1$ since $1/B > 1$ and $1/BC > 1$, the conditions that are relevant to this problem. After the $u=1$ entry site Eq. (33) can manifest two qualitatively different dependencies of f_u on $u-m$. These differences are highlighted by considering the derivative of the relative site probability with respect to $u-m$:

$$\frac{\partial f_u}{\partial(u-m)} = \left[\left(\frac{1}{B} - 1\right)(1 - e^{-\beta qFa}) - \left(\frac{1}{BC} - 1\right)\right] \times e^{(u-m-1)(\beta qFa)}(\beta qFa), \quad (34)$$

where it has been recalled that $A \equiv \exp(\beta qFa)$. In the low-field limit, $F \rightarrow 0$, the second term in the square brackets dominates. Then, with $1/BC > 1$, f_u falls with increasing u and decreasing m. By contrast, the first term in the square brackets can dominate with a sufficiently strong electric field. Then, with $1/B > 1$, f_u rises with increasing u and decreasing m. In particular, charge accumulations on chain sites then increase with decreasing m, $\partial f_u/\partial m < 0$, provided that

$$1 - e^{-\beta qFa} > \frac{\left(\frac{1}{BC} - 1\right)}{\left(\frac{1}{B} - 1\right)}. \quad (35)$$

Upon introducing the definitions of $B \equiv \exp(-\beta\Delta/2)(r/R_f)$ and $C \equiv \exp(-\beta\Delta/2)\ (R/r)$, and noting the relevant physical conditions (see below in Sec. IV), $R_f \geqslant R \geqslant r$ and $\Delta \geqslant 0$, it becomes evident that the condition of Eq. (35) can be satisfied at high fields if r is sufficiently small:

$$1 > \frac{r}{R} e^{\beta\Delta/2}. \quad (36)$$

When this condition is fulfilled current-induced charge redistribution shifts from being bulk limited to being interface limited as the strength of the current-driving electric field is increased. As illustrated in Fig. 2, there is a concomitant qualitative shift in the pattern of charge accumulation at

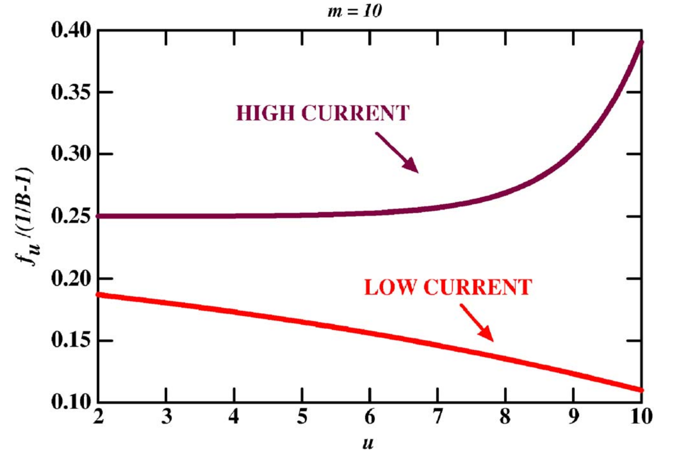

FIG. 2. (Color online) Steady-state flow of carriers from the left drives nonuniform accumulation of small polarons within their m-member chain. With low currents the small-polaron accumulation tends to fall with distance from the site at which carriers enter the small-polaron chain. High currents drive the accumulation to peak where carriers exit the m-member chain. This accumulation typically increases the small-polaron density by a factor $\sim(R_f/r)$ beyond its equilibrium value. The function f_u denotes the current-driven increase of the small-polaron density at site u on the m-site chain divided by its equilibrium value. This function, as given by Eq. (33), divided by $(1/B-1)$ is plotted against u for $\ln A=0.1$ and 1.0 with $(1/BC-1)/(1/B-1)=1/4$ for a 10-site chain. The parameters A, B, and C are defined in terms of the three intersite transition rates in the introductory paragraph of Sec. III.

sites along the m-member chain. In the low-field regime, current-induced charge accumulation occurs most markedly at the site at which carriers *enter* the region where transport is governed by small-polaron hopping. The steady-state charge accumulation then falls with the distance into the m-member chain, u. In the high-field regime, current-induced charge accumulation occurs most markedly at the site at which carriers *exit* the region where transport is governed by small-polaron hopping. The steady-state charge accumulation then increases with the distance into the m-member chain, u.

IV. NUMERICAL ESTIMATES

The current-induced increase in carrier density can become quite large. Consider first the bulk contribution to the fractional current-induced enhancement of the local carrier density, the third contribution on the r.h.s. of Eq. (33). This contribution rises with the ratio of the rate characterizing nearest-neighbor intersite motion of quasifree carriers, R_f, to the rate characterizing nearest-neighbor hopping of small polarons, R. The quasifree nearest-neighbor rate, R_f, is that characterizing the motion of a thermalized quasifree carrier between neighboring sites, $(2kT/m_e)^{1/2}/a \sim 2(kTW)^{1/2}/h$, where W is the electronic bandwidth $W \sim h^2/2m_e a^2$, m_e is the effective mass of the quasifree carrier and a is the nearest-neighbor separation. By contrast, the largest possible rate for thermally activated small-polaron motion is that for adiabatic motion, $R \approx \nu \exp(-\beta W_H)$, where ν is the characteristic vibration frequency and W_H is the activation energy of the small-polaron hopping mobility.[28,29] Thus, the ratio $R_f/R \approx [2(kTW)^{1/2}/h\nu]\exp(\beta W_H)$ is typically very large. This ratio is about 10^4 at room temperature for $W_H = 0.15$ eV and $W = 3$ eV.

The interface contribution to the fractional current-induced enhancement of the local carrier density, the second term on the r.h.s. of Eq. (33), rises with the ratio R_f/r. This ratio is even larger than R_f/R since $R \gg r$. In particular, in the semiclassical regime being considered here $r \ll \nu \exp(-E_{conversion}/kT)$, where $E_{conversion} \gg E_b \gg W_H$. The activation energy $E_{conversion}$ is the deformational energy needed to establish an energy coincidence between the electronic energies of the self-trapped and quasifree states.[30,31] This activation energy rises from its minimum value as the kinetic energy associated with confining a carrier on a single site increases. The associated *barrier to self-trapping* is a general feature that arises from having a finite electronic bandwidth.[21,23–25] These features result in relatively slow conversion between quasifree and self-trapped states, $R \gg r$. This slow conversion rate produces a large interface-related enhancement of the small-polaron density.

The above estimates of R and r ignore the dependences of these rates on the strength of the applied electric field. As noted below Eq. (20), the activation energy of R is increased by $(qFa)^2/8E_b$ upon the application of an electric field.[26] Similar considerations show that the minimum activation energy of r is increased by $(qFa)^2/4E_b$. The theory of adiabatic small-polaron hopping gives $E_b > 2W_H$.[28] The smallest experimental determination of W_H is 0.15 eV.[12–16,20] Taking E_b to be its smallest value and assuming $F = 10^6$ V/cm, a large value, yields maximal corrections to the activation energies that are ~ 0.02 eV when a is as large as 1 nm. Such small corrections to the activation energies are ignorable. In particular, these electric-field dependent corrections to the activation energies are comparable to their experimental uncertainties and are no greater than the room-temperature thermal energy, 0.025 eV. Most importantly, the relative relation $R_f \gg R \gg r$ is unaffected by the application of the external electric field.

Beyond the factors R_f/R and R_f/r, the relative enhancement also depends on $\exp(\beta\Delta)$ and $\exp(\beta\Delta/2)$, respectively. Thus, a significant value of $\beta\Delta > 1$ increases the current-induced accumulation of self-trapped carriers even further. A positive value of Δ ensures that quasifree carriers are stabilized in the crystalline state. It is then the disorder of the noncrystalline state that is presumed to stabilize carriers as small polarons.[32]

Thus, with $(R_f/R)\exp(\beta\Delta) \gg 1$ and $(R_f/r)\exp(\beta\Delta/2) \gg 1$, the density of small polarons will be greatly enhanced as βqFa rises toward a significant fraction of unity. Indeed, typical values indicate that βqFa will rise to about unity with electric-field strengths comparable to those associated with threshold switching. For example, with $a = 0.6$ nm, βqFa will rise from 2.4×10^{-2} to 2.4 at room temperature as the electric field strength is raised from 10^4 V/cm to 10^6 V/cm.

This current-driven local enhancement increases a small-polaron density that already may be relatively large. In particular, with small-polaron transport, current is carried by a relatively high-density of low-mobility carriers rather than by the low-density of high-mobility carriers which characterizes transport in conventional insulators and semiconductors. Since the activation energy of the small-polaron Hall mobility μ_{Hall} is about 1/3 that of its drift mobility μ, $\mu \approx \mu_{Hall} \exp(-2W_{Hall}/kT)$, where W_{Hall} is the Hall mobility activation energy.[18,19,28,29] The small-polaron mobility is thus estimated to be about 10^{-3} cm^2/Vs at 300 K for chalcogenide glasses in which the Hall mobility has been measured.[12,13,15,16]

The equilibrium density of small polarons is given by $n_0 \approx a^{-3} \exp(-\beta E_S)$, where E_S is the characteristic energy of the Seebeck coefficient.[18] For example, analysis of steady-state electronic transport in noncrystalline As_2Te_3 indicates $E_S \approx 0.25$ eV.[12,13] Thus, the equilibrium carrier density in noncrystalline As_2Te_3 is about 10^{18} cm^{-3} at room temperature. A similar analysis in noncrystalline Sb_2Te_3, a much more conducting material, yields $E_S \approx 0.10$ eV and a room-temperature carrier density of about 10^{20} cm^{-3} (Ref. 16).

V. DENSITY-DRIVEN SMALL-POLARON DESTABILIZATION

The efficacy of the electron-lattice interaction in stabilizing small-polarons decreases with their density.[23] In particular, forces exerted by localized self-trapped charge carriers tend to cancel one another in displacing intervening atoms. Thus, there is an upper limit to the fraction of sites upon which charge carriers can self-trap as small polarons. All carriers remain quasifree above this critical density.

To illustrate destructive interference between the atomic displacements arising from adjacent small polarons, consider a chain of sites within the generalized Holstein model. The atomic-strain energy of the atomic-displacement parameters associated with these two sites is $\kappa\Sigma_i x_i^2/2$, where κ is the Hooke's law stiffness constant and x_i is the atomic displacement parameters associated with site i. The electron-lattice interaction depicts the dependence of the potential energies of an electron centered at site i on the atomic-displacement parameters:

$$V_i = -Gx_i + g(x_{i-1} + x_{i+1}). \quad (37)$$

With G and $g > 0$, a carrier on a site induces an expansion of that site's atomic-displacement parameter and a contraction of the neighboring site's atomic-displacement parameter. Minimizing the sum of the electronic potential energy and the atomic strain energy yields the corresponding ground-state energies. The ground-state energy for a single small polaron is $-E_b$, *where* $E_b=(G^2+2g^2)/2\kappa$. However, the ground-state energy for a pair of small polarons on adjacent sites is $-[(G-g)^2+g^2]/\kappa = -2E_b+2Gg/\kappa$. Thus, destructive interference reduces the small-polaron binding energy of the pair from that for two independent small polarons by $2Gg/\kappa$. This simple model illustrates how destructive interference arising from adjacent small polarons can lower their net binding energy. Through this effect, the driving force for carriers to self-trap is reduced by increasing their density.

The stability condition for small-polaron formation can be described by

$$\frac{E_b}{2W} > \frac{1-\alpha_{disorder}}{1-n/n_c}, \quad (38)$$

where E_b is the small-polaron binding energy in the low-density limit and W is the electronic bandwidth. The numerator on the r.h.s. of Eq. (38) indicates that the imposition of disorder, as represented by an increasing positive value of the disorder parameter $\alpha_{disorder}$, fosters a carrier's localization and its collapse into a small polaron.[32] The denominator on the r.h.s. of Eq. (38) indicates that small-polaron formation is destabilized by increasing the small-polaron density n toward a critical value n_c beyond which small-polaron formation is impossible.[23] The condition for a single carrier added to an ordered insulator forming a stable small polaron is given by Eq. (38) with its r.h.s. equal to unity.[21–25]

VI. THRESHOLD SWITCHING

Small polarons can be locally destabilized by a sufficiently large current-induced enhancement of their density. As illustrated in Fig. 2, the current-driven enhancement of the steady-state small-polaron density is not uniform. In particular, with a large enough exit-conversion-limited steady-state current, in accord with Eq. (36), the density of small polarons peaks where they exit the m-member chain. Small polarons at the end of the chain will be destabilized if their density n there is large enough to satisfy the destabilization criterion

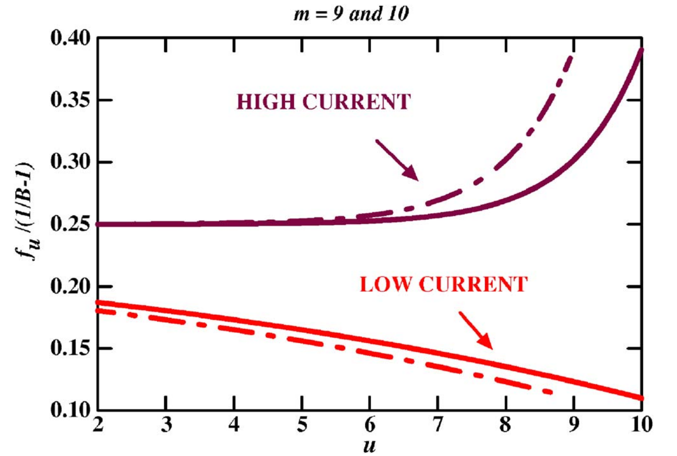

FIG. 3. (Color online) A sufficiently strong current can drive the local density of small polarons high enough to destabilize them with respect to forming quasifree carriers. This effect is modeled as reducing the length of the chain on which carriers self-trap to form small polarons. As depicted above, reducing the chain length from 10 sites (solid lines) to 9 sites (dotted-dashed lines) alters the pattern of small-polaron accumulation. The accumulation driven by a low current is reduced as the chain of sites with small-polaron formation is shortened. By contrast, the small-polaron density driven by a high current rises as the value of m is reduced. These effects are illustrated by plotting f_u, the current-driven increase of the small-polaron density at site u divided by its equilibrium value, for $m=10$ (solid lines) and $m=9$ (dotted-dashed lines) with both low and high currents. The plot shows f_u, as given by Eq. (33), divided by $(1/B-1)$ plotted against u for $\ln A=0.1$ and 1.0 with $(1/BC-1)/(1/B-1)=1/4$. In the introductory paragraph of Sec. III, the parameters A, B, and C are defined in terms of three rates characterizing carriers' intersite motion.

$$\frac{E_b}{2W} < \frac{1-\alpha_{disorder}}{1-n/n_c}. \quad (39)$$

The chain of sites that support small-polaron formation will thereby be shortened.

As illustrated by the uppermost curve of Fig. 3, shortening of the chain of sites supporting small-polaron formation does not reduce the peak small-polaron density. As a result, the shortened chain is itself unstable with respect to further shrinking. Thus, there will be a sequential destabilization and progressive shortening of the chain of sites that support small-polaron hopping. This current-driven shrinkage will continue as an avalanche until the high-resistivity chain is reduced to a small remnant (see Sec. VIII). Concomitantly the resistance will drop as regions with small-polaron hopping are replaced with low resistance regions in which carriers move with high mobility.

These findings are consistent with observations of "threshold switches," summarized in Fig. 4. In particular, threshold switching occurs as the applied *emf* across the region with small-polaron hopping is pushed to a sufficiently high value for the steady-state small-polaron density to exceed its critical value. Then, after a temporal delay during which the system relaxes toward the steady-state conditions associated with the enhanced *emf*, switching to the "on

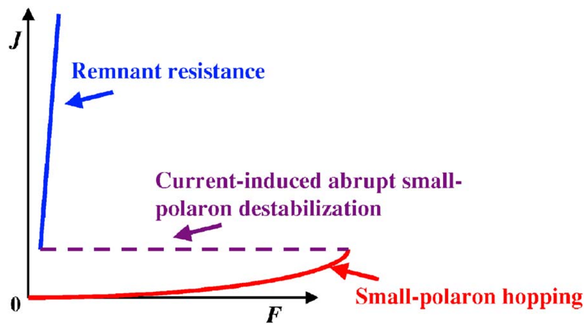

FIG. 4. (Color online) A plot of the current density J versus applied electric field F is used to describe the small-polaron model of threshold switching. An applied electric field drives high-mobility charge carriers into a material in which they form small polarons and move via low-mobility hopping. As the applied field is increased the small-polaron mobility rises exponentially and small polarons increasingly accumulate in the material. Beyond a threshold current, the density of small polarons is driven high enough so that they are destabilized with respect to their forming quasifree carriers. The region with small polarons then shrinks to a small remnant. The resistance of the remnant contributes to that of the high-conductivity state. Reducing current in the high-conductivity state below its "holding" value permits carriers to relax into small polarons thereby reforming the low-conductivity state. Alternatively, current flow in the high-conductivity state may be high enough and prolonged enough to induce a structural phase (e.g., amorphous to crystalline) transition. The switch becomes a memory switch as its maintenance no longer requires a holding current.

state" occurs. By switching, the region without quasifree transport shrinks to just a remnant. The on-state resistance may then be dominated by that of the remnant. In this case, as is often observed, the on-state resistance is independent of the sample thickness.[3] The on state can be maintained with adequate current flow. However, a sufficient reduction of the current will enable the carriers to relax thereby reforming as small-polarons. Thus, a threshold switch returns to its off state if current flow in the on state falls below its "holding" value for a sufficient time.

As indicated by Eq. (33), the electric-field strength is the only externally controlled electronic parameter upon which the current-driven enhancement of the small-polaron density depends. Thus, threshold switching is initiated when the electric-field rises to a material-dependent critical strength $F_{threshold}$. Furthermore, as indicated below Eq. (20) the current density associated with small-polaron hopping at these high electric fields is proportional to $\sinh(\beta qFa/2)$. At high fields this dependency approaches $\exp(\beta qFa/2)$. This dependency is qualitatively consistent with measurements showing current densities and carrier mobilities of chalcogenide glasses rising with applied field as $\exp(D\beta qFa)$, where $D \approx 5-10$.[33–35] However, the measured values of D are significantly larger than that given above for the hopping of independent charge carriers. Subsidiary experiments rule out space-charge effects, contact effects, and Joule heating as the causes of these enhancements.[33–35] Percolation effects, local field corrections, and carriers' mutual interactions may potentially explain these discrepancies.[35]

VII. MEMORY SWITCHING

If the holding voltage for a threshold switch drops to zero, the switch is termed a "memory" switch. The material will then remain in its on state even in the absence of current flow. An appropriately engineered current pulse can return the material from its high-conductivity on state to its low-conductivity off state.[1–3]

The off state and the on state of a memory switch comprise distinct structural phases of the switched material. In the case of chalcogen memory switches, the on state is crystalline while the off state is noncrystalline.

Changing the electronic state of a material can induce structural phase transitions. Such situations are commonly envisioned as consequences of transitions between semiconductorlike electronic behavior and conductorlike electronic behavior in transition-metal oxides.[3] In particular, sustaining a high density of delocalized high-mobility charge carriers can induce an amorphous material's transformation to a crystalline state. Consistent with Eq. (39), the quasifree electronic transport of the crystalline state tends to be stabilized by the lifting of disorder, $\alpha_{disorder} \rightarrow 0$. Sufficient current flow can thereby transform some low-conductivity noncrystalline materials into high-conductivity crystalline phases with quasifree charge carriers.

Reports that continued current flow through the on state of a threshold switch precedes crystallization are consistent with this picture.[1–3] The similarity of the electrical behavior of the on states of threshold and memory switches is also consistent with the crystallization of a memory switch being electrically driven, rather than being thermally driven.[1–3]

The on state crystalline phase of a memory switch can be returned to an off state noncrystalline phase. In particular, Joule heating can be used to melt crystalline material. Subsequent rapid cooling of the melt can leave it in its noncrystalline state. Since the electric field in the crystalline on state is small, see Fig. 4, the resulting charge carriers will be in their low-conductivity off state.[1–3]

VIII. DISCUSSION

This paper has presented an electronic mechanism for driving a small-polaron semiconductor into a high-conductivity state. The conductivity transition of the small-polaron semiconductor occurs when the density of small polarons is pushed so high that they are destabilized with respect to forming free carriers. This accumulation of small polarons is propelled by high-mobility charge carriers being driven into a semiconductor within which they form small polarons and move with their characteristically low hopping-type mobility.

A significant disparity between rates associated with charge-carrier transport to, into, through, and from the small-polaron semiconductor is required to produce a suitably configured current-driven accumulation of small polarons to presage the conductivity transition. High-mobility quasifree charge carriers move rapidly between adjacent atomic sites with the rate R_f. Small polarons hop slowly between adjacent sites of the semiconductor with the rate R. The very slow rate r characterizes the carriers' conversion between being quasi-

free and being small polarons at the semiconductor's two interfaces. When $R_f \gg R \gg r$, a sufficiently strong current will produce a nonuniform accumulation of small polarons that peaks where carriers exit the semiconductor. When driven to a sufficiently high density, this spatial distribution of small polarons becomes unstable with respect to their near-global conversion into quasifree carriers.

The present work has only explicitly addressed the motion of the predominant charge carriers (e.g., small-polaron holes in binary chalcogenide glasses). Nonetheless, this paper's arguments can be extended to address a semiconductor with both electronlike and holelike small polarons. With a sufficiently strong driving field, small polarons with opposing signs will be driven toward opposing ends of the sample, here the *m*-member chain. The widths of each of these two peaks of accumulated charge will be $\sim kT/qF$. The current-driven shrinkage of the chain with small-polaron charge carriers will cease when the peaks of the oppositely signed accumulated charge overlap. Then the accumulated densities of oppositely charged carriers will tend to diminish as the overlapping carriers recombine with one another. Thus, the current-driven shrinking of the low-conductivity chain will leave a small remnant region of width $\sim kT/qF$. Indeed, measurements of the resistance of the high-conductivity state of the switched material are consistent with it being dominated by a small remnant.[1–3] In particular, the resistance of the high-conductivity state of switched material is found to be independent of sample thickness.[1–3]

This work demonstrates how current-driven charge accumulation can drive threshold switching. Proceeding beyond the present independent-carrier treatment to include space charge effects would require treating Coulomb interactions between all charge centers. Recombination between oppositely charged carriers should then also be explicitly considered. Inclusion of energetic and transfer-energy disorder in treating small-polaron hopping would require study of a multidimensional model so as not to exaggerate their percolative effects. However, inclusion of these effects, a very formidable task, would not essentially alter the idea that sufficient current-driven accumulation of small polarons destabilizes them with respect to their forming quasifree charge carriers.

[1] D. Adler, *CRC Critical Reviews in Solid State Sciences*, (CRC Press, New York, 1971), Vol. 2.
[2] D. Adler, H. K. Henisch, and N. Mott, Rev. Mod. Phys. **50**, 209 (1978).
[3] N. F. Mott and E. A. Davis, *Electronic Processes in Non-crystalline Materials* (Clarendon Press, Oxford, 1979), Chap. 9.13, p. 512.
[4] E. Weintraub, J. Indus. Engin. Chem. **5**, 106 (1913).
[5] F. W. Lyle, Phys. Rev. **11**, 253 (1918).
[6] J. H. Bruce and A. Hickling, Trans. Faraday Soc. **35**, 1436 (1939).
[7] K. Moorjani and C. Feldman, in *Boron and Refractory Borides*, edited by V. I. Matkovich (Springer-Verlag, Berlin, 1977), pp. 581–596.
[8] C. F. Drake, I. F. Scanlan, and A. Engel, Phys. Status Solidi B **32**, 193 (1969).
[9] S. R. Ovshinsky, Phys. Rev. Lett. **21**, 1450 (1968).
[10] O. A. Golikova, Phys. Status Solidi A **101**, 277 (1987).
[11] I. G. Austin and N. F. Mott, Adv. Phys. **18**, 41 (1969).
[12] D. Emin, C. H. Seager, and R. K. Quinn, Phys. Rev. Lett. **28**, 813 (1972).
[13] C. H. Seager, D. Emin, and R. K. Quinn, Phys. Rev. B **8**, 4746 (1973).
[14] C. H. Seager and R. K. Quinn, J. Non-Cryst. Solids **17**, 386 (1975).
[15] G. R. Klaffe and C. Wood, in *Physics of Semiconductors: Proceedings of the 13th International Conference on the Physics of Semiconductors*, International Union of Pure and Applied Physics, edited by F. G. Fumi (North-Holland Publishing Company, London, 1976), pp. 545–548.
[16] S. A. Baily and D. Emin, Phys. Rev. B **73**, 165211 (2006).
[17] D. Emin, Philos. Mag. **35**, 1189 (1977).
[18] D. Emin, *Electronic and Structural Properties of Amorphous Semiconductor*, edited by P. G. LeComber and J. Mort (Academic Press, London, 1973), Chap. 7, pp. 261–328.
[19] D. Emin, *The Hall Effect and its Applications*, edited by C. L. Chien and C. R. Westgate (Plenum Press, New York, 1980), pp. 281–298.
[20] S. A. Baily and D. Emin, Solid State Commun. (to be published).
[21] Y. Toyozawa, Prog. Theor. Phys. **26**, 29 (1961).
[22] D. Emin, Phys. Rev. Lett. **28**, 604 (1972).
[23] D. Emin, Adv. Phys. **22**, 57 (1973).
[24] D. Emin and T. Holstein, Phys. Rev. Lett. **36**, 323 (1976).
[25] N. F. Mott and A. M. Stoneham, J. Phys. C **10**, 3391 (1977).
[26] D. Emin, Adv. Phys. **24**, 305 (1975).
[27] D. Emin, Phys. Rev. Lett. **32**, 303 (1974).
[28] D. Emin and T. Holstein, Ann. Phys. (N.Y.) **53**, 439 (1969).
[29] D. Emin in Phys. Today **35**, 34, 1982.
[30] D. V. Lang and C. H. Henry, Phys. Rev. Lett. **35**, 1525 (1975).
[31] C. H. Henry and D. V. Lang, Phys. Rev. B **15**, 989 (1977).
[32] D. Emin and M.-N. Bussac, Phys. Rev. B **49**, 14290 (1994).
[33] H. J. de Wit and C. Crevecoeur, J. Non-Cryst. Solids **8-10**, 787 (1972).
[34] J. M. Marshall and G. R. Miller, Philos. Mag. **27**, 1151 (1973).
[35] I. G. Austin in *Linear and Nonlinear Electronic Transport in Solids*, edited by J. T. Devresse and V. E. van Doren (Plenum Press, New York, 1976), pp. 383–409.